Influence of Aging and Thermomechanical Treatments on the Mechanical Properties of a Nanocluster-Strengthened Ferritic Steel

Z.W. ZHANG, C.T. LIU, Y.R. WEN, A. HIRATA, S. GUO, G. CHEN, M.W. CHEN, and BRYAN A. CHIN

This study investigated the effect of aging and thermomechanical treatments on the mechanical properties of a nanocluster-strengthened ferritic steel, Fe-1.5Mn-2.5Cu-4.0Ni-1.0Al (wt pct). The effect of thermomechanical treatments on the microhardness and tensile properties were measured at room temperature and correlated with microstructural features. Cu-rich precipitates were characterized by transmission electron microscopy and were found to coarsen slowly during long-time aging. The microhardness measurements indicate a typical precipitation hardening behavior during aging at 773 K (500 °C). Tensile tests showed that thermomechanical treatments can improve the mechanical strength and ductility of the nanocluster-strengthened ferritic steel significantly compared with those without the treatments. Fractography results indicated that the high yield strength resulted from precipitation hardening makes the steel more susceptible to grain-boundary decohesion, which can be suppressed by grain refinement. Atmosphere adsorption and diffusion along grain boundaries were found to intensify brittle intergranular fracture, and this embrittlement can be avoided by vacuum heat treatment.

DOI: 10.1007/s11661-011-0835-4

I. INTRODUCTION

PRECIPITATION strengthening of steels by Cu-rich nanoscale precipitates is of great commercial importance because the low carbon content of these strong steels results in improved ductility and weldability.[1–5] The Cu additions can compensate for the decrease in strength from reducing the C concentration through precipitation of Cu-rich nanoclusters.[4,5] The low-carbon with copper-addition steels, such as high strength low-alloy (HSLA) steels, were initially developed by the U.S. Navy for use in the construction of the hulls of ships and submarines.[6,7] Because of their high strength, good impact toughness, and excellent weldability, these steels are also of interest to the transportation, civil infrastructure, and defense industries for applications such as vehicle frames for heavy duty trucks, oil pipelines, offshore drilling platforms, bridges, military vehicles, *etc*.[3,8–12]

Previous research on HSLA steel plates showed that the quenching, tempering and aging processes were needed to produce martensitic steels containing Cu precipitates. The combination of the strength and toughness of these steels was obtained by tempered lath martensite structures along with somewhat overaged Cu precipitates.[3,11–13] Recent research on Cu-rich nanocluster strengthened steels indicated that body-centered-cubic (bcc) Cu-rich nanoclusters are coherent with the steel matrix and provide significant precipitation strengthening. As a result, the processes of martensite formation and subsequent tempering are no longer required.[14–16] The strength of the Cu-rich nanocluster strengthened ferritic steels is derived mainly from nanocluster precipitation strengthening, which can be readily controlled by aging processes. The bcc Cu-rich precipitates can prevent dislocation movement through changing the screw dislocation core energy as the dislocation traverses the precipitates,[17,18] which effectively improve the yield strength.[4]

However, it is well known that with an increase in hardness, alloys become more susceptible to intergranular embrittlement. The influence of the yield strength is particularly important in high-strength steels because intergranular decohesion is stress controlled, so the higher the yield strength, the more severe is the

Z.W. ZHANG, Research Fellow, is with the Materials Research & Education Center, Auburn University, Auburn, AL 36849, and also a Lecturer, with the Engineering Research Center of Materials Behavior and Design, Ministry of Education, Nanjing University of Science and Technology, Nanjing 210094, P. R. China. C.T. LIU, Distinguished Professor, is with the Materials Research & Education Center, Auburn University, and also a Professor, with the MEEM Department, College of Science and Engineering, City University of Hong Kong, Kowloon, Hong Kong. Contact e-mail: chainliu@cityu.edu.hk Y.R. WEN, Doctoral Student, A. HIRATA, Assistant Professor, and M.W. CHEN, Professor, are with the WPI Advanced Institute for Materials Research, Tohoku University, Sendai 980-8577, Japan. S. GUO, Research Fellow, formerly with the Department of Mechanical Engineering, the Hong Kong Polytechnic University, Kowloon, Hong Kong, is now with the MEEM Department, College of Science and Engineering, City University of Hong Kong. G. CHEN, Professor, is with the Engineering Research Center of Materials Behavior and Design, Ministry of Education, Nanjing University of Science and Technology. BRYAN A. CHIN, Professor, is with the Materials Research & Education Center, Auburn University.

Manuscript submitted February 21, 2011.

Published online: 27 July 2011

embrittlement caused by the grain-boundary decohesion.[19,20] The strong obstacle to dislocation glide by nanoscale Cu-rich precipitates keeps the matrix strength high. This increases the possibility of grain-boundary decohesion under a high stress with an attendant potential to increase the likelihood of brittle fracture.[21] Moreover, oxygen in air has been identified as the harmful species responsible for the embrittlement in the precipitation-strengthened alloys[22] and in several other alloy systems.[18,23–26] The absorption of H_2O and O_2 in air can generate atomic oxygen through surface reaction during high-temperature heat treatments. The absorbed oxygen then diffuses into the alloy interior along grain boundaries and intensifies the grain-boundary cohesion.[26] The benefits of grain refinement in suppressing the grain-boundary decohesion are well known. Thermomechanical treatment (TMT) has achieved a desired microstructure tailored to the specific mechanical properties of HSLA steels.[3,13] By adopting the TMT techniques, it is possible to obtain a fine-grained microstructure with an excellent combination of strength and ductility. However, few attempts have been made to study the influence of TMT on the structure and properties of Cu-rich, nanocluster-strengthened ferritic steel.[27] In this study, the effects of aging and TMT on a recently developed Cu-rich, nanocluster-strengthened ferritic steel[27] were investigated. The effect of atmosphere-induced grain-boundary decohesion of this steel was also evaluated.

II. EXPERIMENTAL

A. *Alloy Preparation*

Ingots with a nominal composition of 1.5Mn, 2.5Cu, 4.0Ni, 1.0Al (wt pct), and balanced α Fe were prepared by arc-melting high-purity elemental metals (99.95 Fe, 99.8 Mn, 99.99 Ni, 99.99 Cu, 99.99 Al wt pct). The ingots were remelted several times to ensure homogeneous distribution of the alloying elements under a Ti-gettered Ar atmosphere. The arc-melted alloy button was then drop-cast into rods of 10 mm in diameter. The chemical composition of the as-cast steels is shown in Table I.

The concentrations of C and S in the steel were determined by combustion-infrared absorbance; the concentration of N was determined by inert gas fusion-thermal conductivity and the concentrations of other elements were determined by inductively coupled plasma (ICP) atomic emission spectroscopy according to ASTM Standard E 1019-08.

B. *Thermomechanical Treatments*

To evaluate the effect of TMT on the microstructure and mechanical properties, two processing routes with and without TMT were selected. Following the processing routes without TMT, the as-cast specimens were heated at 1273 K (1000 °C) in air for 1 hour, followed by quenching in water. The as-quenched specimens were aged at 773 K (500 °C) in air for 1 to 200 hours, respectively. For TMT processing, the as-cast ingots were annealed at 1273 K (1000 °C) in air for 1 h and then hot-rolled using a pilot plant rolling mill to a final thickness of about 6 mm through two passes. After rolling, the steel plates were water quenched immediately. The hot rolled specimens were then cold rolled to a final thickness of about 1 mm using multiple passes. The rolling ratio was approximately 20 pct per pass for a total thickness reduction of approximately 80 pct. The cold-rolled specimens were held at 1173 K (900 °C) for 30 minutes in air and then quenched into water. The as-quenched specimens were then aged at 773 K (500 °C) in air for various times (specimen TMT1). To evaluate the effect of the heat-treatment atmosphere on the mechanical properties and fracture mode, some cold-rolled plates were selected for heat treatment in vacuum. Specifically, the cold-rolled plates were cut into tensile specimens first by electrodischarge machining (EDM). The as-cut tensile specimens were heated and held at 1173 K (900 °C) for 30 minutes in an induction vacuum furnace with vacuum level of ~2×10^{-2} Pa. The specimens were then furnace cooled in vacuum to 823 K (550 °C) and held at this temperature for 2 hours (specimen TMT2). For comparison, other as-cut tensile specimens were held at 1173 K (900 °C) in air for 30 minutes and then quenched into water. The as-quenched specimens were aged at 823 K (550 °C) for 2 hours in air (specimen TMT 3). The heat treatments of the specimens with and without TMT are summarized in Table II.

C. *Testing and Characterization*

Sheet tensile samples with gage sizes of $12.5 \times 3 \times 0.75$ mm were prepared by EDM and were carefully polished to remove the damaged surface layers. Tensile tests were performed on an Instron 5565 testing machine at room temperature in air. Tensile specimens were tested at a strain rate of 0.04 seconds^{-1}. Three samples were tested, and an average experimental value from the three samples was reported. The yield strength was determined using the 0.2 pct offset plastic strain method. Hardness measurements were conducted under a 500 g applied load, and the average hardness (VHN) of 10 measurements from different locations was reported.

Optical microscopy (OM), scanning electron microscopy (SEM) and transmission electron microscopy (TEM) were used to characterize the microstructure of the specimens. The OM and SEM samples were mechanically polished to a final particle size of 0.2 μm and then etched for approximately 10–20 seconds with a 4 vol pct Nital solution. The grain size was determined

Table I. Chemical Composition of the As-Cast Steel (Weight Percent)

C	Si	Mn	P	S	Cu	Ni	Al	N	Fe
0.01	<0.01	1.42	<0.005	0.002	2.49	4.14	1.00	0.003	bal.

Table II. Treatment Schemes of Nanocluster-Strengthened Ferritic Steel

Specimen	Solution	Aging	Atmosphere
Without TMT	1273 K (1000 °C)/1 h	773 K (500 °C)/various times	air
TMT1	1173 K (900 °C)/30 min	773 K (500 °C)/various times	air
TMT2	1173 K (900 °C)/30 min	823 K (550 °C)/2 h	vacuum
TMT3	1173 K (900 °C)/30 min	823 K (550 °C)/2 h	air

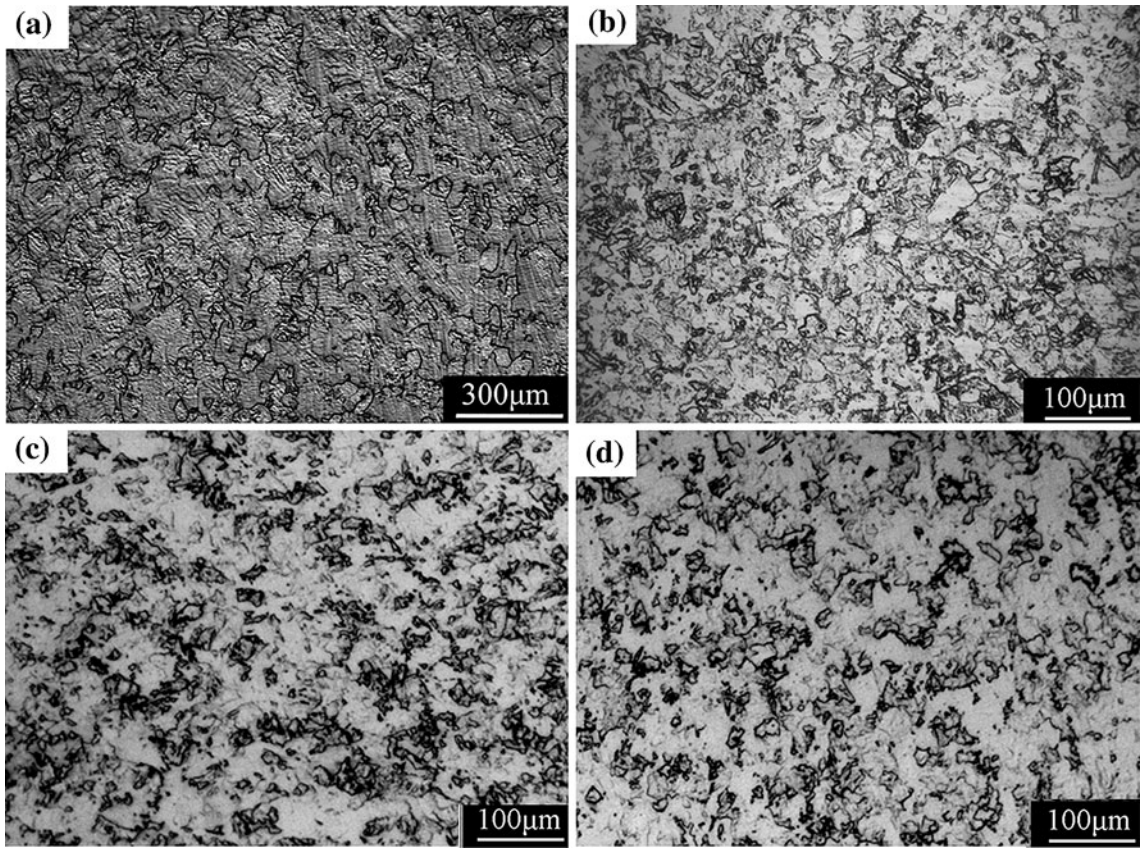

Fig. 1—Optical microstructures of (*a*) as-cast steel after aging at 773 K for 1 h (without TMT); (*b*) TMT steel after aging at 773 K (500 °C) for 1 h (TMT1); (*c*) TMT steel after aging at 823 K for 2 h in vacuum (TMT2); and (*d*) TMT steel after aging at 823 K (550 °C) for 2 h in air (TMT3). Note: The steel without TMT was annealed at 1273 K (1000 °C) for 1 h in air and then quenched into water before aging; TMT1 and TMT 3 steels were annealed at 1173 K (1000 °C) for 30 min in air and quenched into water before aging; TMT 2 steel was annealed at 1173 K (900 °C) for 30 min and furnace cooled to aging temperature in vacuum before aging.

by linear interception method. The fracture surfaces were examined using a JEOL 7000F SEM (JEOL Ltd, Tokyo, Japan) operated at 20 kV. TEM samples were prepared by using twin-jet electropolishing in 5 pct HClO4 methanol solution followed by ion milling at 2 kV, 2 mA, and 10 °C for 30 min. Philips CM12 120 kV (Philips Electronics, Amsterdam, The Netherlands) and JEOL 2100F with double Cs-corrector 200 kV were employed for the characterization of the nanoclusters. Both models are actually TEMs.

III. RESULTS AND DISCUSSION

A. *Optical Microstructure*

Figure 1 shows the optical microstructures of the specimens with and without TMT. Cellular and skeletal-like cast structures are clearly visible in the as-cast steel after water-quenching and aging at 773 K (500 °C) for 1 hour (see Figure 1(a)). The average grain size was approximately 50 μm. Prolonging the aging time any more does not change the optical microstructure. After thermomechanical treatment, the grain size was refined significantly. As can be observed from Figure 1(b), the grain size of specimen TMT1, which was aged at 773 K (500 °C) for 1 hour after water-quenching from 1173 K (900 °C), was reduced to approximately 10 μm. Prolonging the aging time did not change the optical microstructure significantly. Aging at 823 K (550 °C) for 2 hours in either air or vacuum did not affect the grain size significantly compared to aging at 773 K (500 °C) for 1 hour. The grain sizes of the specimen TMT2 and TMT3 are similar to that of TMT1 (see Figures 1(b) through (d)).

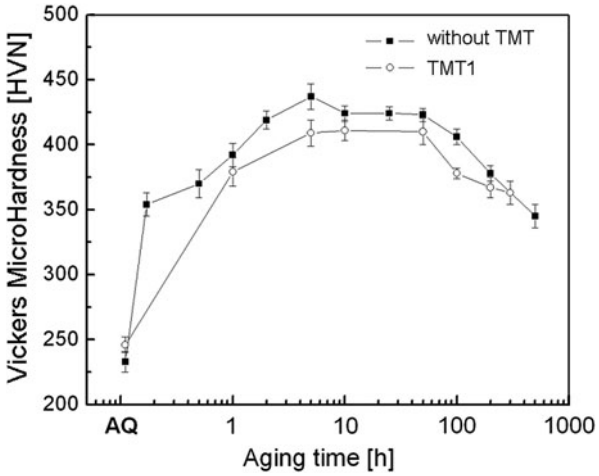

Fig. 2—Microhardness as a function of aging time. The aging process of both steel without TMT and TMT1 steels was carried out at a fixed temperature of 773 K (500 °C) in air.

B. *Effect of Aging on Microhardness*

Figure 2 shows the microhardness test results of specimen without TMT and TMT1 as a function of aging time. The aging process was fixed at a temperature of 773 K (500 °C). It is obvious that for both steels with and without TMT, there was a low VHN value in the as-quenched condition. The VHN was increased significantly after aging even for a short time. The hardness increased with an increase in aging time and reached the maximum of ~436 and ~411 HVN at the aging time of 5 hours for the specimen without TMT and 10 hours for TMT1 specimen, respectively. The hardness curves demonstrate a hardness plateau for both the steel without TMT and TMT1 steels from an aging time of 10–50 hours. The hardness decreased again with another increase in aging time beyond 50 hours at 773 K (500 °C), indicating the overaging had occurred. The hardness of the steel with TMT was found to be lower compared with the steels without TMT after aging at 773 K (500 °C) from 1 hour through 200 hours. The lower hardness of TMT steels, compared with the steels without TMT, is probably induced by the breakdown of the large skeleton structures by thermomechanical treatments (see Figure 1).

The microhardness changes with aging time at the same aging temperature are mainly to the result of Cu-nanocluster precipitation and then coarsening. Figure 3 shows the nanocluster precipitation and evolution with the aging time. Aging for 1h, extensive and homogeneous nucleation of Cu-rich nanoclusters with an average size of ~2 nm occurs (Figure 3(a)), resulting in a significant increase of microhardness compared with the as-quenched specimen. After aging for 10 hours, the Cu-rich nanoclusters grow slightly to an average size of ~5 nm (Figure 3(b)). The appropriate size and density of the nanoclusters for blocking dislocation movement, along with possibly increased lattice strains between the Cu-rich nanoclusters and Fe matrix, causes another improvement in the microhardness. Upon aging for 500 hours, obvious coarsening along with the dramatic density decrease of the nanoclusters can be observed. The coarsened nanoclusters have an average size of ~10 nm. Preliminary HRTEM characterization (the insert of Figure 3(c)) indicates that the coarsened nanoclusters in the aged sample aged for 500 hours seem to remain the lattice coherency with the bcc matrix. However, the coarsening of the precipitates leads to a decrease of hardness.

C. *Tensile Properties*

Figure 4 shows the ultimate tensile strength (UTS) and yield strength (YS) *vs* aging time. Tensile tests were performed at room temperature in air. Each data point represents the average of several tests. It can be observed from Figure 4 that the UTS and YS for the steels with TMT show a trend that is similar to the microhardness. The UTS and YS of the TMT steels increased significantly after aging at 773 K (500 °C) for 1 hour. The UTS increased from 637 MPa after water-quenching to 1157 MPa after aging at 773 K (500 °C) for 1 hour and the YS increased from 457 MPa to 1063 MPa. Beyond the aging peak of 5 hours, the UTS and YS decreased with subsequent aging time, showing a typical dependence of the Cu-rich precipitates on aging time again. However, it is obvious from Figure 4 that the UTS and YS of the steels without TMT behave differently from those of the TMT steels with aging time. In the water-quenched condition and after aging at 773 K (500 °C) for 200 hours, the UTS and YS of the steels without TMT behave similar to the microhardness of the TMT steels. However, after aging at 773 K (500 °C) for 1 hour and 10 hours, the UTS of the steels without TMT decreased significantly compared with those of the TMT steels. These steels without TMT fractured prior to macroscopic yielding and no yield strength was obtained. This difference indicates clearly that TMT is beneficial to hindering the brittle fracture.

Figure 5 shows the ductility profile of the steels with and without TMT after aging at 773 K (500 °C) for various periods. It can be observed from Figure 5 that the plastic elongation of the steels is influenced significantly by the aging time and thermomechanical treatments. In the water-quenched condition, the plastic elongation of the TMT steels is approximately 23 pct, which is much higher than that of the specimens without TMT (13 pct). With subsequent aging, the plastic elongation of both steels with and without TMT decreased significantly. This is because of the Cu-rich nanoparticles hindering the dislocation movement.[2] However, it is obvious from Figure 5 that the plastic elongations of the TMT samples were higher than those of the steels without TMT for all aging times in this study. For the TMT samples, the plastic elongation reached a minima of about ~1.5 pct at an aging time of 5 hours. Increasing the aging time to 200 hours, the elongation of the TMT steel increased to ~10 pct because of the coarsening of Cu-rich nanoclusters.[28,29] However, the plastic elongation of the specimens without TMT decreased sharply to 0 after aging at 773 K (500 °C) for 1 hour, showing a brittle fracture. With

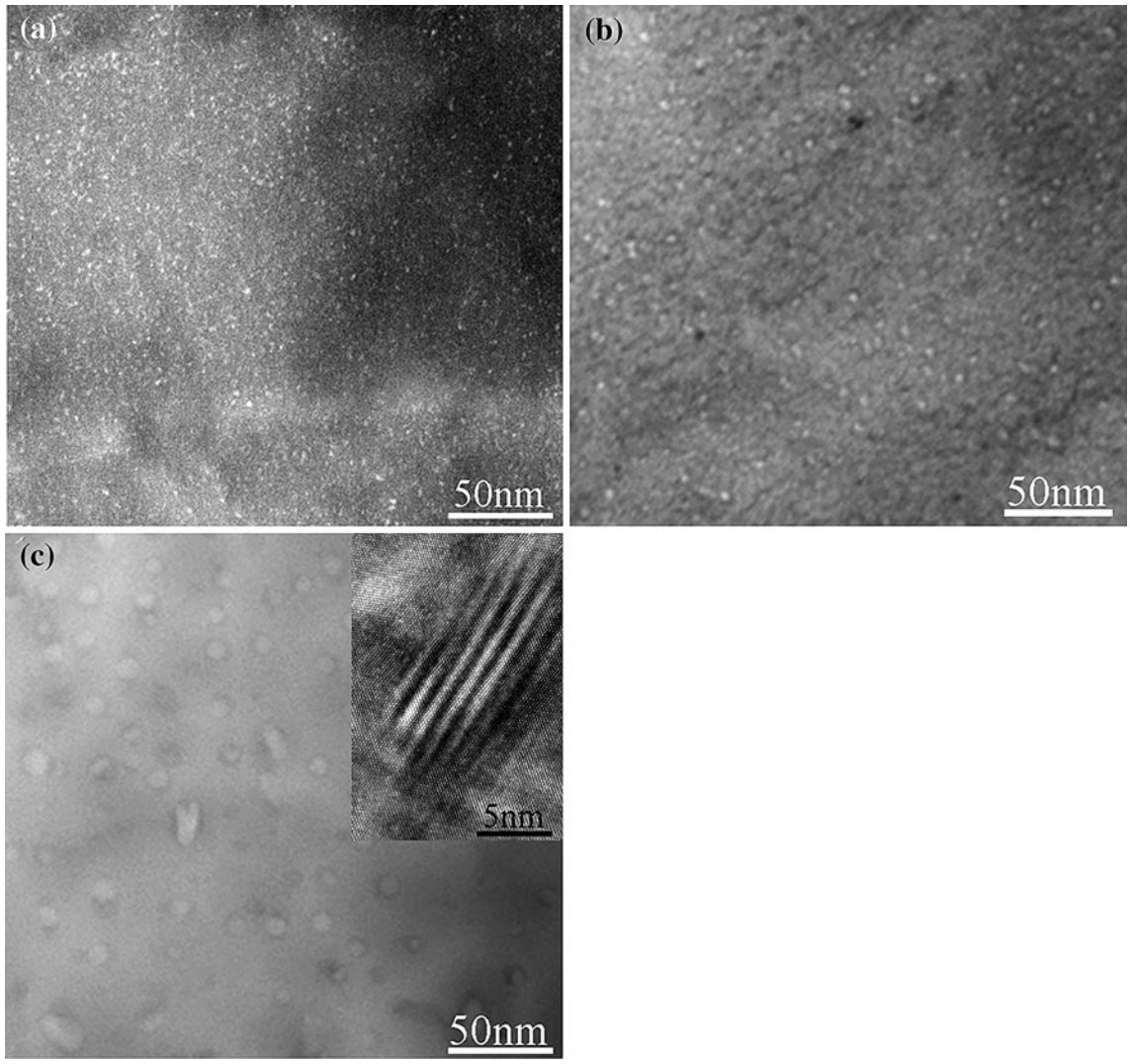

Fig. 3—TEM image showing nanocluster precipitation and evolution as a function of aging time in the samples without TMT: (*a*) aging for 1 h (*b*) aging for 10 h, and (*c*) aging for 500 h. Bright points in the pictures represent nanoclusters. HRTEM image shows a typical Cu precipitate which seem to be coherent with the bcc matrix.

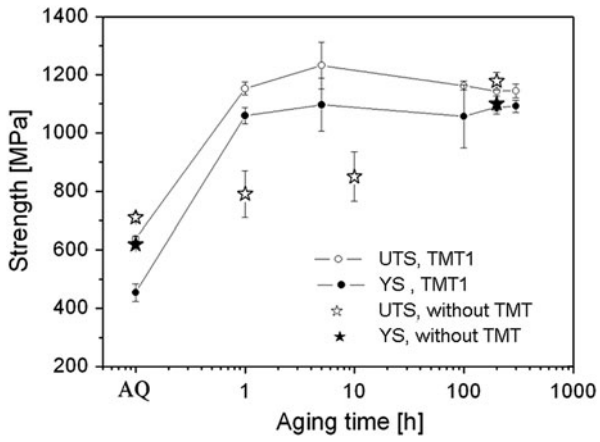

Fig. 4—Ultimate tensile strength and yield strength as a function of aging time. Aging process of both the steels without TMT and TMT1 steels was carried out at a fixed temperature of 773 K (500 °C) in air. The yield strengths of the steels without TMT after aging for 1 h and 10 h were not determined because the steels fractured prior to macroscopic yielding.

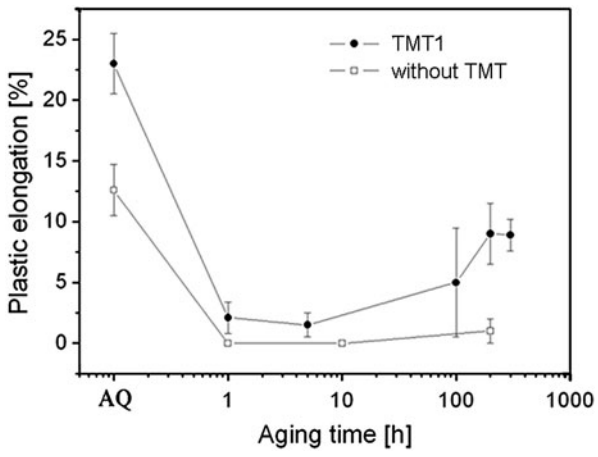

Fig. 5—Plastic elongation as a function of aging time. Aging process of both the steels without TMT and TMT1 steels was carried out at a fixed temperature of 773 K (500 °C) in air.

increasing aging times up to 200 hours, no significant improvement in plasticity was observed.

D. *Fracture Mode*

To explore the effect of aging and thermomechanical treatment on the fracture mode, the failed tensile samples were examined by SEM. The results of these investigations on the steels without TMT and TMT1 steels are shown in Figure 6. As can be observed in this figure, the thermomechanical treatment does not affect the fracture mode of the steels considerably after water quenching. Both steels with and without TMT shows a microvoid coalescence rupture, indicating a ductile fracture. However, TMT does affect the fracture mode significantly when the specimens were water-quenched and aged at 773 K (500 °C) for 1 hour and 200 hours. After water quenching and aging at 773 K (500 °C) for 1 hour, the fractography of the specimen without TMT reveals a combination of intergranular and cleavage facets, indicating a brittle fracture, whereas the TMT specimen fails by a quasi-cleavage pattern. After aging at 773 K (500 °C) for 200 hours, the specimens with and without TMT have distinctly different fractographies.

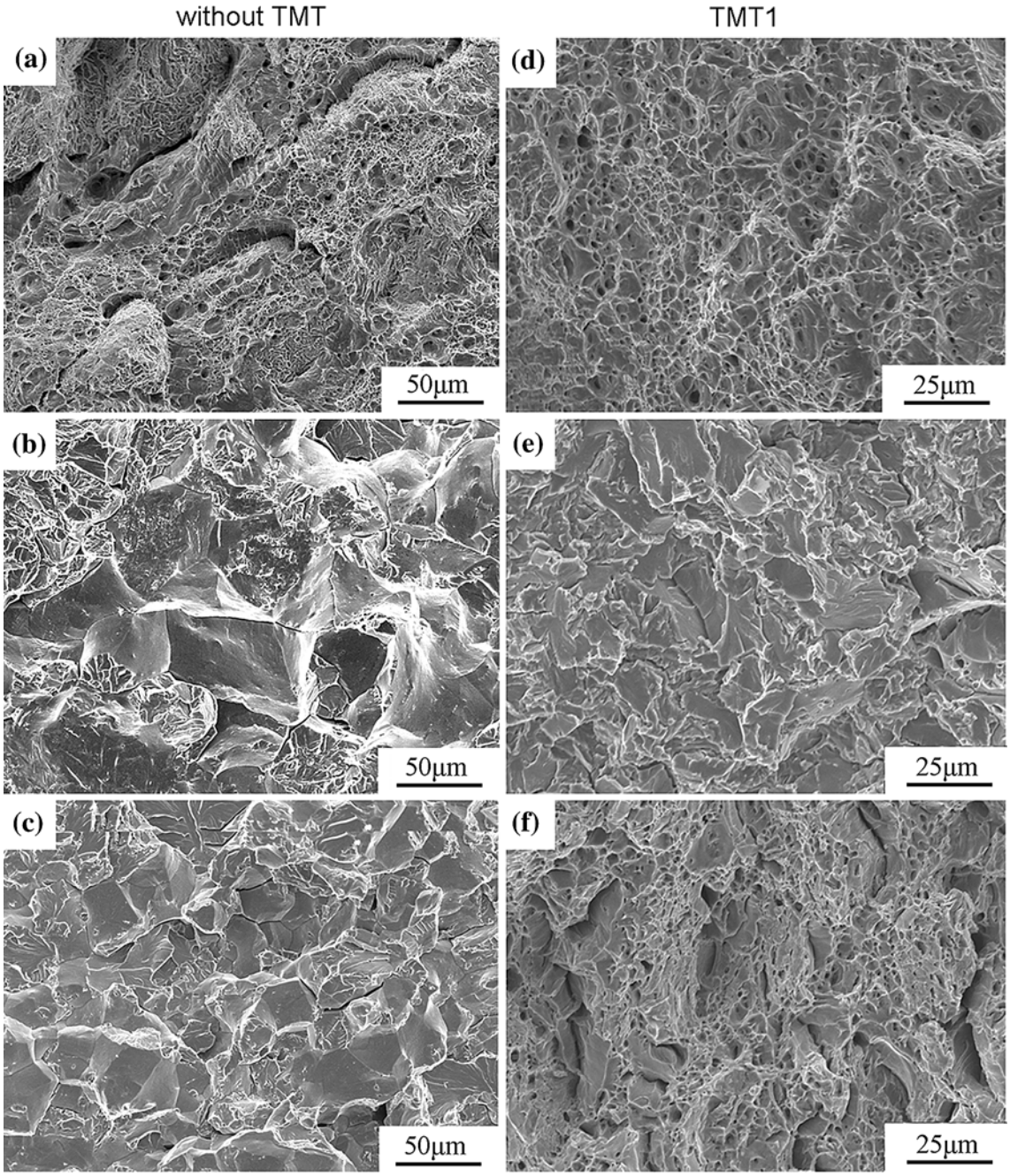

Fig. 6—Fracture surfaces of the steels with and without TMT after aging at 773 K (500 °C) in air for (*a*) As quenched, without TMT; (*b*) without TMT, 1 h; (*c*) without TMT, 200 h; (*d*) TMT1-as quenched; (*e*) TMT1, 1 h; and (*f*) TMT1, 200 h.

The fractography of the TMT specimen shows a microvoid coalescence fracture mode, whereas the specimen without TMT shows a combination of intergranular and cleavage facets, similar with that of the sample aged at 773 K (500 °C) for 1 hour.

It is apparent from the tensile test results and fracture surfaces that for the as-quenched sample, the strength is found to be lower because of the absence of Cu-rich nanoprecipitates strengthening compared with aged samples. In this case, both the samples with and without TMT shows the similar microvoid coalescence rupture. After aging, the yield strength of the samples with and without TMT increased significantly because of precipitation strengthening. The high yield strength makes the steels more susceptible to intergranular embrittlement. As shown in Figure 6, for the specimens without TMT, the fracture surfaces of both the samples aged for 1 hour and 200 hours at 773 K (500 °C) are mainly dominated by intergranular rupture, leading to a low ductility. In contrast, all the TMT steels show a transgranular fracture and higher ductility compared with the specimens without TMT. This certainly suggests that grain refinement obtained by TMT can effectively suppress grain boundary decohesion and enhance the ductility of the steels.

For TMT steels, after aging at 773 K (500 °C) for 1 hour, the fractography reveals a quasi-cleavage pattern while a microvoid coalescence fracture mode after aging for 200 hours was observed though they have the similar strength (see Figure 4). This indicates that the nanocluster size and density affect the fracture mode. The small size along with a high density of the Cu-rich nanoclusters obtained with short aging time tends to result in a quasi-cleavage pattern while overaged large size along with lower density of these clusters tends to form a microvoid coalescence fracture mode. Thus, by varying the thermomechanical parameters and heat treatment, the microstructure can be controlled, and the mechanical properties can be enhanced to a great extent by effectively making use of these varied microstructures and Cu-rich precipitates. Indeed, thermomechanical treatment has been applied widely to enhance the mechanical properties of HSLA steels.[30,31]

E. *Effect of Heat Treatment Environment on the Ductility*

Figure 7 compares the tensile properties of the TMT specimens heat-treated in vacuum (TMT2) and in air (TMT3), respectively. Tensile tests of the specimens of TMT2 and TMT3 were carried out under the same testing conditions. Both samples have the similar yield strength whereas the ductility of TMT 3 is much lower than that of TMT2. The maximum elongation of TMT2 is approximately 16 pct, whereas TMT3 is only ~1.4 pct and fails in a brittle manner. Both the TMT2 and TMT3 steels showed the same hardness of ~384 HVN, which is consistent with the measured yield strength. The difference in mechanical properties between the TMT2 and TMT3 specimens is apparently not induced by the Cu-rich nanoclusters, but the heat treatment atmospheres. Figure 8 shows the fracture surfaces of the specimen TMT2 and TMT3. It can be observed that the processing atmospheres significantly affect the fracture mode.

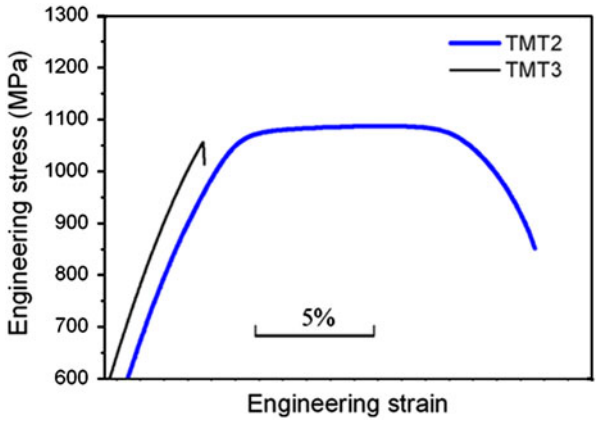

Fig. 7—Engineering stress *vs* engineering strain curves for TMT2 and TMT3 steels. TMT2 represents the thermomechanically treated steels, which were aged at 823 K (550 °C) for 2 h in vacuum after heating at 1173 K (900 °C) for 30 min in vacuum; TMT3 represents the thermomechanically treated steels, which were aged at 823 K (550 °C) for 2 h in air after heating at 1173 K (900 °C) for 30 min in air. The curves have been displaced along the *x* axis for the sake of better visibility.

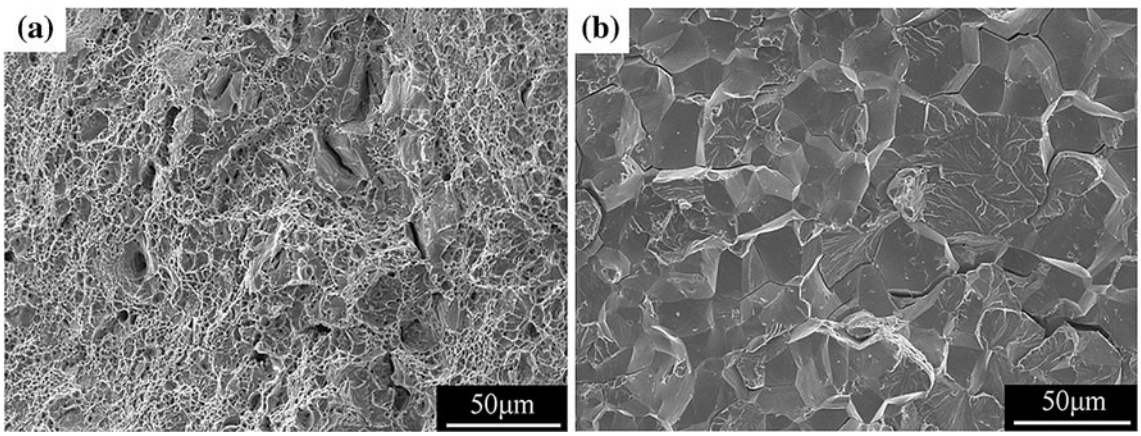

Fig. 8—Fracture surfaces of the (*a*) TMT2 steel and (*b*) TMT3 steel.

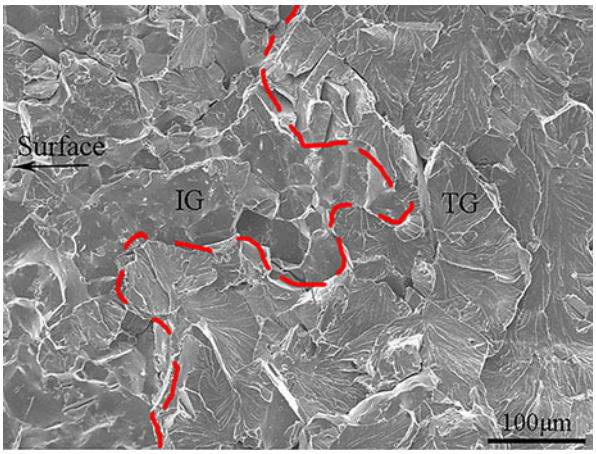

Fig. 9—Fracture surfaces of the steels without TMT. The samples were heated at 1273 K (1000 °C) in air for 1 h and then quenched in water. The as-quenched specimen was aged at 773 K (500 °C) in air for 200 h. The picture shows that near the sample surface, the fracture surface is dominated by intergranular fracture. In the alloy interior, the fracture mode changed from intergranular (IG) to transgranular (TG).

Heat treatment in a vacuum leads to the sample failure by a microvoid coalescence mode (see Figure 8(a)), whereas the specimens heat treated in air fail in a brittle mode mainly by intergranular fracture mixed with some cleavage facets.

To identify the underlying mechanisms of the atmosphere-induced embrittlement, the fracture surfaces of the samples heat-treated in air were carefully characterized. Figure 9 shows a typical fracture surface of the sample without TMT. The sample was first annealed at 1273 K (1000 °C) in air for 1 hour and then aged at 773 K (500 °C) in air for 200 hours after quenched by water. The fractograph shows that the region near the sample surface is dominated by intergranular fracture while the center part of the sample fails by cleavage. This suggests that the embrittlement caused by the heat treatment in air is associated with the grain boundary weakening, which is most likely induced by oxygen adsorption and diffusion along grain boundaries.[20,32–35] Figure 7 shows clearly that with heating at 1173 K (900 °C) in air, the sample exhibits a brittle stress-strain curve with limited plasticity. While heating at 1173 K (900 °C) in vacuum, the sample presents a ductile stress-strain behavior, indicating that atmosphere-induced embrittlement can be avoided by the vacuum heat treatment.

IV. CONCLUSIONS

The effects of aging and thermomechanical treatments on the mechanical properties of a nanocluster-strengthened ferritic steel were investigated. After water-quenching and aging, a cellular and skeletal-like cast structure with an average grain size of about 50 μm are visible in the as-cast steel whereas the thermomechanically treated samples have an equiaxed grain structure with a grain size of about 10 μm. TEM results show that extensive and homogeneous nucleation of Cu-rich nanoclusters with an average of ~2 nm occurs after aging for 1 hour at 773 K (500 °C). The Cu-rich nanoclusters grow slightly to an average size of ~5 nm after aging for 10 hours and finally coarsen to ~10 nm along with a dramatic density decrease after aging for 500 hours. The microhardness as a function of aging time for both samples with and without TMT shows a typical precipitation hardening behavior during aging at 773 K (500 °C). Tensile tests demonstrate that TMT can improve the yield strength and ductility of the ferritic steel significantly. Fractography results indicate that the high yield strength resulted from precipitation hardening makes the steel more susceptible to grain-boundary decohesion. The adsorption of oxygen in air and diffusion of oxygen along grain boundaries enhance the embrittlement based on previous studies.[22,32–34] Grain refinement obtained by TMT can effectively suppress grain boundary decohesion, and the atmosphere-induced embrittlement can be avoided by vacuum heat treatment.

ACKNOWLEDGMENTS

This research was supported mainly by internal funding from Auburn University, Hong Kong City University, and together with the NJUST Research Funding (No. 2010GIPY031) and the National Natural Sciences Foundation of China (No. 50871054). Z.W.Z. benefitted from the Visiting Postdoctoral Research Program at the Neutron Scattering Science Division, Oak Ridge National Laboratory, Oak Ridge, TN.

REFERENCES

1. H.R. Habibi Bajguirani: *Mater. Sci. Eng. A*, 2002, vol. 338, pp. 142–59.
2. S. Vaynman, D. Isheim, R.P. Kolli, S.P. Bhat, D.N. Seidman, and M.E. Fine: *Metall. Mater. Trans. A*, 2008, vol. 39A, pp. 363–73.
3. S.K. Dhua, D. Mukerjee, and D.S. Sarma: *Metall. Mater. Trans. A*, 2003, vol. 34A, pp. 241–53.
4. M.E. Fine and D. Isheim: *Scripta Mater.*, 2005, vol. 53, pp. 115–18.
5. D. Isheim, M.S. Gagliano, M.E. Fine, and D.N. Seidman: *Acta Mater.*, 2006, vol. 54, pp. 841–49.
6. E.J. Czyryca, R.E. Link, R.J. Wong, D.A. Aylor, T.W. Montemarano, and J.P. Gudas: *Nav. Eng. J.*, 1990, vol. 102, pp. 63–82.
7. A.D. Wilson: *J. Metals*, 1987, vol. 39, pp. 36–38.
8. S.W. Thompson, D.J. Colvin, and G. Krauss: *Metall. Mater. Trans. A*, 1996, vol. 27A, pp. 1557–71.
9. M.T. Miglin, J.P. Hirth, A.R. Rosenfield, and W.A.T. Clark: *Metal. Trans. A*, 1986, vol. 17A, pp. 791–98.
10. S.W. Thompson, D.J. Colvin, and G. Krauss: *Metal. Trans. A*, 1990, vol. 21A, pp. 1493–1507.
11. S.K. Dhua, D. Mukerjee, and D.S. Sarma: *Metall. Mater. Trans. A*, 2001, vol. 32A, pp. 2259–70.
12. S.K. Dhua, A. Ray, and D.S. Sarma: *Mater. Sci. Eng. A*, 2001, vol. 318, pp. 197–210.
13. G.C. Hwang, S. Lee, J.Y. Yoo, and W.Y. Choo: *Mater. Sci. Eng. A*, 1998, vol. 252, pp. 256–68.
14. S. Vaynman, M.E. Fine, S. Lee, and H.D. Espinosa: *Scripta Mater.*, 2006, vol. 55, pp. 351–54.
15. S. Vaynman, D. Isheim, M.E. Fine, D.N. Seidman, and S.P. Bhat: *2004 Conf. Proc.*, vol. 1. New Orleans, LA, AIST and TMS, 2004, pp. 525–30.

16. D. Isheim and D.N. Seidman: *Surf. Interface Anal.*, 2004, vol. 34, pp. 569–74.
17. T. Harry and D.J. Bacon: *Acta Mater.*, 2002, vol. 50, pp. 209–22.
18. J.H. Shim and Y.W. Choo: *Appl. Phys. Lett.*, 2007, vol. 90, p. 021906.
19. W.M. Kane, U. Krupp, and C.J. McMahon: *Mater. Sci. Eng. A*, 2009, vol. 507, pp. 58–60.
20. C.J. McMahon: *Interface Sci.*, 2004, vol. 12, pp. 141–46.
21. S.B. Fisher, J.E. Harbottle, and N. Aldrige: *Phil. Trans. R. Soc. Lond. A*, 1985, vol. 315, pp. 301–32.
22. W.M. Kane, U. Krupp, and C.J. McMahon: *Mater. Sci. Eng. A*, 2009, vol. 507, pp. 61–65.
23. C.T. Liu and C.L. White: *Acta Metall.*, 1987, vol. 35, pp. 643–49.
24. C.T. Liu, C.L. White, and E.H. Lee: *Scripta Metall.*, 1985, vol. 19, pp. 1247–50.
25. M. Takeyama and C.T. Liu: *Mater. Sci. Eng. A*, 1992, vol. 153, pp. 538–47.
26. R. Zee, C. Yang, Y.X. Lin, and B. Chin: *J. Mater. Sci.*, 1991, vol. 26, pp. 3853–61.
27. J.H. Zhu and C.T. Liu: *Intermetallics*, 2002, vol. 10, pp. 309–16.
28. Z.W. Zhang, C.T. Liu, S. Guo, J.L. Cheng, G. Chen, T. Fujita, M.W. Chen, Y.W. Chung, S. Vaynman, M.E. Fine, and B.A. Chin: *Mater. Sci. Eng. A*, 2011, vol. 528, pp. 855–59.
29. M.K. Miller and K.F. Russell: *J. Nucl. Mater.*, 2007, vol. 371, pp. 145–60.
30. A. Machova: *Mater. Sci. Eng. A*, 2001, vol. 319-21, pp. 574–77.
31. S. Sangal and S. Yannacopoulos: *Can. Metall. Q.*, 1992, vol. 31, pp. 55–61.
32. B. Hwang and C.G. Lee: *Mater. Sci. Eng. A*, 2010, vol. 527, pp. 4341–46.
33. X.M. Deng, F.S. Ma, and M.A. Sutton: *Int. J. Damage Mech.*, 2005, vol. 14, pp. 101–26.
34. C.T. Liu, R.W. Carpenter, and H. Inouye: *Metall. Trans. A*, 1975, vol. 6A, pp. 419–21.
35. U. Krupp, W.M. Kane, C. Laird, and C.J. McMahon: *Mater. Sci. Eng. A*, 2004, vol. 387, pp. 409–13.